Proc. Natl. Acad. Sci. USA
Vol. 93, pp. 1864–1869, March 1996
Physiology

Antisense oligodeoxynucleotide inhibition of a swelling-activated cation channel in osteoblast-like osteosarcoma cells

RANDALL L. DUNCAN*†, NEIL KIZER*, ELIZABETH L. R. BARRY‡, PETER A. FRIEDMAN‡, AND KEITH A. HRUSKA*§

*Renal Division, Jewish Hospital, Washington University Medical Center St. Louis, Missouri 63110; and ‡Department of Pharmacology & Toxicology, Dartmouth Medical School, Hanover, NH 03755

Communicated by David M. Kipnis, Washington University School of Medicine, St. Louis, MO, October 25, 1995

ABSTRACT **By patch-clamp analysis, we have shown that chronic, intermittent mechanical strain (CMS) increases the activity of stretch-activated cation channels of osteoblast-like UMR-106.01 cells. CMS also produces a swelling-activated whole-cell conductance (G_m) regulated by varying strain levels. We questioned whether the swelling-activated conductance was produced by stretch-activated cation channel activity. We have identified a gene involved in the increase in conductance by using antisense oligodeoxynucleotides (ODN) derived from the α_1-subunit genes of calcium channels found in UMR-106.01 cells (α_{1S}, α_{1C}, and α_{1D}). We demonstrate that α_{1C} antisense ODNs abolish the increase in G_m in response to hypotonic swelling following CMS. Antisense ODNs to α_{1S}, and α_{1D}, sense ODNs to α_{1C}, and sham permeabilization had no effect on the conductance increase. In addition, during cell-attached patch-clamp studies, antisense ODNs to α_{1C} completely blocked the swelling-activated and stretch-activated nonselective cation channel response to strain. Antisense ODNs to α_{1S} treatment produced no effect on either swelling-activated or stretch-activated cation channel activity. There were differences in the stretch-activated and swelling-activated cation channel activity, but whether they represent different channels could not be determined from our data. Our data indicate that the α_{1C} gene product is involved in the G_m and the activation of the swelling-activated cation channels induced by CMS. The possibility that swelling-activated cation channel genes are members of the calcium channel superfamily exists, but if α_{1c} is not the swelling-activated cation channel itself, then its expression is required for induction of swelling-activated cation channel activity by CMS.**

Mechanical strain increases bone formation and remodeling activity resulting in a net increase in bone mass (1–3). However, the mechanisms by which the osteoblasts and other bone-forming cells sense mechanical stimuli and transduce biochemical signals have yet to be identified. We previously characterized a mechanosensitive, cation nonselective channel in osteoblast-like cells (4) that is modulated by parathyroid hormone (5). These channels are not voltage regulated; they are dihydropyridine insensitive, and they are inhibited by the trivalent gadolinium (Gd^{3+}). We hypothesize that these channels act as signal transducers for the anabolic effects of mechanical strain and parathyroid hormone. Application of chronic, intermittent mechanical strain (CMS) to osteoblasts increases stretch-activated cation channel open probability and sensitivity of the channel to mechanical strain as well as eliciting spontaneous channel activity (6). Spontaneous channel activity and identification of a component of cell conductance due to stretch-activated cation channel activity had not been previously demonstrated for these channels (7). Application of CMS to osteoblasts also produces an increase in whole-cell conductance (G_m) when the osteoblast is challenged by hypotonic swelling (6). Our observations suggest that, during physical loading of the osteoblast, stretch-activated or swelling-activated cation channels are an integral component of the electrical environment and mediate ion flux into the cell.

Osteoblasts not only respond to CMS by modulating the stretch-activated cation channel, but gene transcription for bone-matrix proteins is altered as well (8). Application of CMS to human osteoblast-like osteosarcoma cells for 24–72 hr increases type I procollagen message and type I collagen secretion. CMS also up-regulates osteopontin message and osteocalcin secretion independent of 1,25-dihydroxyvitamin D_3. Whether the effects of CMS on bone matrix protein expression and production are modulated through the stretch-activated cation channel has not been determined.

Using homology-based reverse transcriptase PCR, Barry *et al.* (9) isolated partial cDNA clones of three α_1 subunits of calcium channels in UMR-106.01 osteoblast-like osteosarcoma cells. They found a unique conservation of alternative splicing across each of the α_1-subunit genes in UMR-106.01 cells, α_{1S}, α_{1C}, and α_{1D} (see ref. 10 for nomenclature). Alternative splicing of α_1 subunit was described by Perez-Reyes *et al.* (25) who found two variants of α_{1S} and four of α_{1C} and α_{1D}. Barry *et al.* (9) found that rodent osteoblast-like cells express only the b variant (Perez-Reyes designation) of all three α_1 subunits. Employing an antisense strategy in the studies reported here, we demonstrate that antisense to the α_{1C} channel subunit is capable of blocking the G_m increase in UMR-106.01 osteoblast-like osteosarcoma cells in response to hypotonic swelling following CMS. Furthermore, the α_{1C} antisense oligodeoxynucleotide (ODN) blocks the single cation channel response to hypotonic strain and stretch activation in cells exposed to CMS.

MATERIALS AND METHODS

Cell Culture. UMR-106.01 cells (passages 12–18) were grown in minimal essential medium with Eagle's modification, nonessential amino acids, and Earle's salts (Sigma) supplemented with 10% fetal bovine serum (GIBCO). Cells were plated onto flexible, type I collagen-coated, silicone-bottomed six-well culture plates (Flexercell, McKeesport, PA), fed twice weekly, and maintained in a humidified atmosphere of 95% air/5% CO_2 at 37°C. When the cells were ≈75% confluent, sense or antisense ODNs were introduced into the cells as described below. To induce CMS, culture plates were placed on an apparatus that uses vacuum to stretch the silicone-bottomed plates. Cyclic stretch was applied for 12–30 hr at

The publication costs of this article were defrayed in part by page charge payment. This article must therefore be hereby marked "*advertisement*" in accordance with 18 U.S.C. §1734 solely to indicate this fact.

Abbreviations: CMS, chronic, intermittent mechanical strain; G_m, whole-cell conductance; ODN, oligodeoxynucleotide; NP_o, open channel activity.

†Present address: Department of Orthopaedic Surgery, Indiana University Medical Center, Clinical Building Suite 600, 541 Clinical Drive, Indianapolis, IN 46202-5111.

§To whom reprint requests should be addressed at: Renal Division, Jewish Hospital of St. Louis, 216 South Kingshighway, St. Louis, MO 63110.

three cycles per min. The strain pattern associated with the Flexercell apparatus is nonuniform (12). Strain E was measured as a fraction of deformation: $E = \Delta l/l$, where l = length of a cell; $\mu E = \mathrm{E} \times 10^6$. The profiles of strain range from 120,000 μE at the edge of the well (12% maximal displacement) to 0 μE at the center. The cells used in this study were subjected to similar magnitudes of strain since patches were always performed in an area 7 mm from the edge of the well. Strain applied to this area was estimated at 80,000–100,000 μE using the strain curve described by Banes *et al.* (12). Comparisons were made between chronically strained control and ODN-treated cells from the same passage number and at the same level of confluence.

Introduction of ODNs. A pair of antisense/sense ODNs (24-mer) and a 20-mer antisense ODN were developed from the sequence of a α_{1C} cDNA of the L-type calcium channel genes isolated from the UMR-106.01 cell line (9) by reverse transcriptase PCR.¶ The sequence of the antisense ODN (24-mer) was 5′-CCTTCCGTGCTGTTGCTGGGCTCA-3′ and that of the sense ODN was 5′-TGAGCCCAGCAACAG-CACGGAAGG-3′. The sequence of the antisense 20-mer was ACTCTGGAGCACACTTCTTG. ODNs were synthesized by MacroMolecular Resources (Fort Collins, CO) and introduced into UMR-106.01 cells using streptolysin O (Sigma) permeabilization (13). After the UMR-106.01 cells had been plated onto flexible silicone-bottomed culture plates and grown to 75% confluence, the medium was removed and the cells were washed with a permeabilization buffer consisting of 137 mM NaCl, 5.6 mM glucose, 2.7 mM KCl, 2.7 mM EGTA, 1 mM NaATP, 100 mM Pipes, 0.1% bovine serum albumin (pH 7.4). The permeabilization buffer containing 0.5 unit of streptolysin O per ml and the appropriate ODN at 100 μM was then placed on the cells for 5 min at room temperature. This solution was then removed and the normal medium with 10% fetal bovine serum was added to the cells. To test the effects of streptolysin alone, UMR-106.01 cells were permeabilized with the same concentration of streptolysin O with no ODN present. These experiments are referred to in the figures and text as "sham permeabilized." Similar procedures were used for application of antisense ODNs to the α_{1S} and α_{1D} isoforms of the α_1 subunits of the L-type calcium channels. Cell membrane permeabilization by the above technique was uniform, nonlethal, and completely reversible as assessed by complete recovery of membrane potential (V_m) and cell resistances following removal of the streptolysin O. The initial V_m of patched untreated cells was -33.8 ± 4.7 mV (range, 21.9–69; $n = 23$), while that of streptolysin O-treated cells was -32.6 ± 3.3 mV (range, 18–70 mV; $n = 51$).

Patch-Clamp Studies. Following application of CMS, the silicone bottom of the cluster was removed and transferred to a recording chamber (1 ml total vol) (Biophysica Technologies, Baltimore), which was modified to permit rapid exchange of the bathing solution with minimal perturbation to the cells. Cells were bathed in a "normal" mammalian Na^+ Ringer's solution consisting of 138 mM NaCl, 5.5 mM KCl, 1 mM $MgCl_2$, 1 mM $CaCl_2$, and 20 mM Hepes buffer titrated to pH 7.3 with NaOH. To impose membrane strain on the UMR cells during the patch-clamp studies, 10 ml of 65 mM NaCl (182 mOsm) hypotonic Ringer's solution was perfused into the chamber. The circumferential strain of a spherical cell can be approximated as $E \approx (d_2\pi - d_1\pi)/d_1\pi$, which simplifies to $E \approx (d_2 - d_1)/d_1$, where d_1 is diameter of a spherical cell prior to swelling and d_2 is the diameter after swelling. This computation assumes even distribution of force across the plasma membrane and no addition of new membrane after swelling. Although many laboratories use hypotonic swelling as a means of imposing mechanical strain on cells, we realize that stretch and swelling are very different and the distinction is maintained throughout this report, which is focused on swelling-induced channel activity in order to analyze the increase in swelling-induced whole-cell conductance (G_m) produced by CMS.

To measure V_m and G_m, the nystatin perforated-patch technique was used under current-clamp conditions (14). The pipette solution in these experiments consisted of 12 mM NaCl, 64 mM KCl, 28 mM K_2SO_4, 47 mM sucrose, 1 mM $MgCl_2$, 0.5 mM EGTA, 20 mM Hepes, titrated to 7.35 with KOH. Nystatin was added at a concentration of 300 μg/ml to permeabilize the patch. Access resistances of <40 MΩ were consistently achieved with this concentration of nystatin. Whole-cell conductance (G_m) measurements were made by pulsing ± 50 pA across the membrane. Acceptable patches for analysis were determined by maintenance of negative cell polarization after returning to isosmotic conditions, the persistence of the large cell membrane capacitive current spike in response to a 20-mV voltage pulse at the beginning and end of the experiment, and the ability to reseal the patch in the outside out configuration. These criteria were used to confirm that the perforated-patch configuration remained intact throughout the experimental period.

Pipette solutions for single channel recordings contained either 144.0 mM KCl, 10.0 mM KHepes, 1.0 mM $MgCl_2$ or 138.0 mM NaCl, 5.5 mM KCl, 1.0 mM $MgCl_2$, 8.0 mM NaHepes in the pipette. To determine the channels' monovalent ion selectivity ratios, bath solutions were exchanged between the normal bathing solution (see above), the high potassium pipette solution, and an isotonic low NaCl solution containing 65.0 mM NaCl, 5.5 mM KCl, 1.0 mM $MgCl_2$, 1.0 mM $CaCl_2$, 8.0 mM NaHepes, and 154.0 mM mannitol. The channels' selectivity to calcium was determined by changing bath solutions between the normal NaCl bathing solution and a high calcium solution containing 75.0 mM $CaCl_2$, 5.5 mM KCl, 1.0 mM $MgCl_2$, 8.0 mM NaHepes, and 60.0 mM mannitol. All bath solutions were maintained at pH 7.3.

Voltage-pulse protocols for construction of current–voltage (I–V) plots consisted of holding inside-out patches at -70 mV referenced to the pipette for 5 sec between 4-sec pulses to holding potentials, which were stepped from -100 or -150 mV to $+100$ or $+150$ mV in 10-mV increments. Electrophysiologic signals were amplified with a List EPC-7 patch-clamp amplifier (Adams–List, Westbury, NY), filtered at 1 kHz with an eight-pole Bessel filter (Frequency Devices, Haverhill, MA), and displayed on a Tektronix oscilloscope. A Digidata 1200 interface (Axon Instruments) was used to digitize the filtered signal, which was stored on the hard drive of a 386DX computer (Dell Computers, Austin, TX). Data were acquired and analyzed using the PCLAMP 6.02 software (Axon Instruments). Cursor measurements were made to determine the magnitude of discrete single-channel openings, and these current magnitudes were plotted against the holding voltage. I–V plots were fitted to the GHK current equation (15) using the nonlinear fitting algorithm in the SIGMAPLOT software program (Jandel Scientific, San Rafael, CA).

Statistical Analysis. The significance of differences between means for the experimental groups was assessed by using the Bonferroni correction (16).

RESULTS

We have previously shown that hypotonic challenge induces a large increase in G_m in UMR-106.01 cells only after the cells have been subjected to CMS (Table 1). This increase in conductance correlates with increased stretch-activated cation channel activity (6) and a similar increase in swelling-activated cation channel activity (figure 3 in ref. 6). Both swelling-activated and stretch-activated cation channel activity and the

¶A patent application has been filed for the discovery described in this publication.

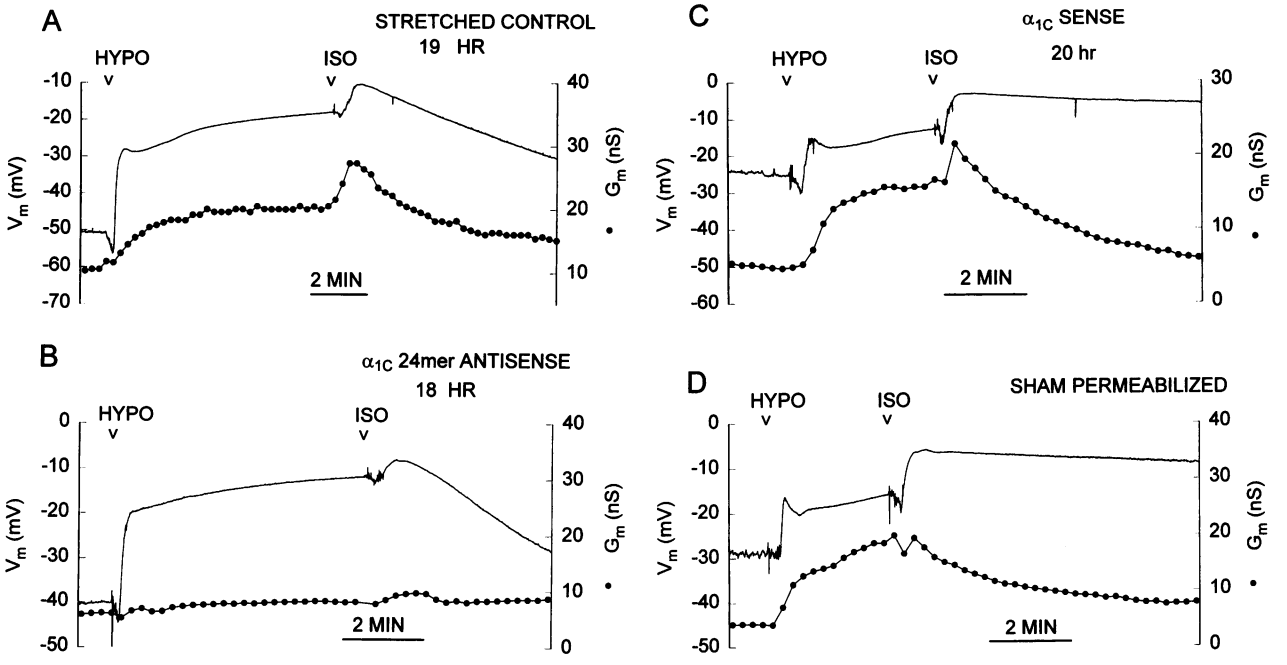

FIG. 1. Effect of an antisense 24-mer ODN from the α_1 subunit of the UMR-106.01 calcium channel 2 gene (α_{1C}) on the response of V_m and G_m to hypotonic stretch. (*A*) UMR-106.01 cell V_m and G_m response to hypotonic stretch (hypo) and reversal in isotonic media (iso). The cells had been exposed to chronic mechanical cyclic strain for 18 hr. (*B*) As in *A*, except the cells had been treated with the α_{1C} antisense ODN during the 19 hr of mechanical strain. Data are representative of several similar experiments (see Table 1). (*C*) Cells were loaded with the sense ODN in parallel with the antisense ODN used 18 hr prior to study, during which time the cells were exposed to chronic cyclic strain as described. (*D*) As in *A*, except the cells were exposed to anti-streptolysin O but no ODN. Data are representative of several similar experiments (see text).

hypotonic challenge-induced conductance are completely inhibited by the stretch-activated cation channel blocker, Gd^{3+} (6). In this study, we examined the effects of antisense ODNs derived from nucleotide sequences of the α_1-subunit isoforms of the calcium channels, α_{1S}, α_{1C}, and α_{1D} on the G_m increase observed after hypotonic challenge of cells exposed to CMS. Antisense ODNs produced a time-dependent inhibition of the chlorothiazide-induced increase in intracellular calcium in mouse distal convoluted tubule cells (17). This inhibition started 6 hr after introduction of the antisense ODN and was maximal at 18 hr. The delay in inhibition was attributed to turnover of existing proteins before inhibition of new synthesis by the antisense ODN. We observed a similar time course of inhibition of CMS-induced increase in swelling-activated cell conductance by the α_{1C} antisense ODNs. Inhibition of the increase in conductance began at 12 hr, and it was maximal at 18–22 hr. G_m measurements of untreated cells, mechanically strained for 18–19 hr, the "stretch control," were increased 71.2% ± 2.7% (n = 21) after hypotonic swelling. Representative experiments are illustrated in (Figs. 1*A* and 2*A*).[‖] There was complete inhibition of the CMS-induced increase in swelling-activated conductance in cells of companion wells treated with α_{1C} antisense ODN (24-mer) (Fig. 1*B*). Blockage of CMS-induced increase in conductance was observed in 18 separate cultures of UMR-106.01 cells. Comparable observations were made using the α_{1C} 20-mer antisense ODN derived from a sequence upstream of the 24-mer ODN. The α_{1C} antisense (20-mer) (n = 7) (Fig. 2*B*) abolished the increase in conductance produced by CMS in the stretched control cells (Fig. 2*A*). UMR-106.01 cells permeabilized with streptolysin O in the absence of ODN, the sham permeabilized, exhibited increased conductance in response to swelling (67.2% ± 5.9%; n = 6) (Fig. 1*D*) with no differences compared to cells not treated with streptolysin O. Introduction of the 24-mer α_{1C} sense ODN had no significant effects on the increase in G_m resulting from hypotonic swelling (n = 4) (Fig. 1*C*). In cells exposed to the α_{1C} antisense ODNs, return of the swelling-activated G_m response was observed after 26 hr. Interestingly, this response was usually greater than the control response (R.L.D. and K.A.H., unpublished data), suggesting a feedback mechanism resulting in increased expression of the channel following recovery from antisense inhibition. Antisense ODNs (24-mers) to the α_1 subunit of two other calcium channel genes (α_{1S} and α_{1D}) of the L-type found in UMR-106.01 cells were also tested. Neither α_{1D} (Fig. 3*A*) nor α_{1S} antisense ODNs (Fig. 3*B*) from the same IVS6 region of the α_1 subunit altered the conductance response to hypotonic swelling in UMR-106.01 cells (n = 6 for both α_{1S} and α_{1D}).

The G_m increase in response to hypotonic swelling following CMS correlates with an increase in stretch-activated cation single channel activity (6) and is blocked by Gd^{3+} (figure 2 in

Table 1. Effects of ODNs on increase in cell conductances produced by hypotonic swelling of UMR-106.01 cells

	Peak change in conductance, nS	No. of experiments
No ODN, no CMS	4.2 ± 0.7	8
No ODN, CMS 18 hr	15.3 ± 1.8*	21
Sham ODN, CMS 18 hr	11.0 ± 1.7	6
α_{1C} 24-mer antisense, CMS 18 hr	2.8 ± 0.7†	18
α_{1C} 24-mer sense, CMS 18 hr	11.6 ± 0.6	4
α_{1C} 20-mer antisense, CMS 18 hr	3.7 ± 0.9†	7
α_{1S} 24-mer antisense, CMS 18 hr	12.3 ± 2.8	6
α_{1D} 24-mer antisense, CMS 18 hr	11.7 ± 1.1	6

Data for peak change in conductance are means ± SEM.
*$P < 0.001$ compared to no ODN, no CMS.
†$P < 0.001$ compared to no ODN, CMS 18 hr. Sham ODN CMS 18 hr cells were exposed to streptolysin O but no ODN.

[‖]The recently described consensus nomenclature for calcium channel subunits is used in this report (10). According to this convention, α_{1S} is the same as CaCh1, α_{1C} is CaCh2, and α_{1D} is CaCh3 (18).

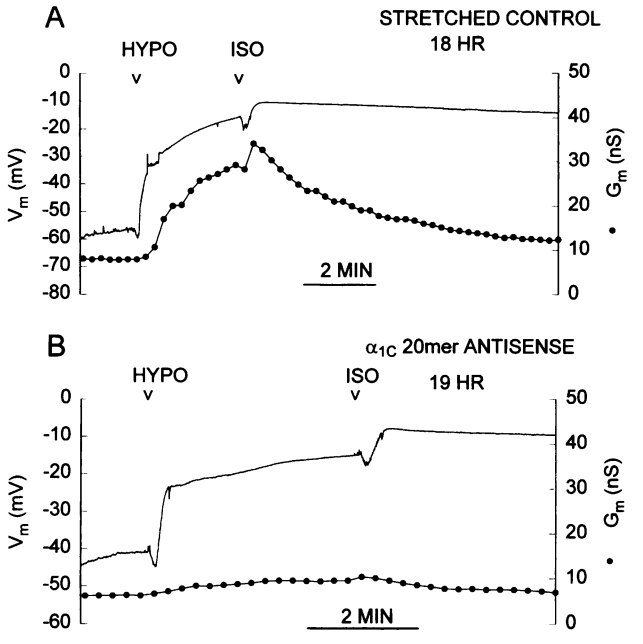

FIG. 2. Effect of an antisense 20-mer ODN from the UMR-106.01 α_{1C} gene on the response to hypotonic stretch. (*A*) UMR-106.01 cells exposed to 18 hr of chronic cyclic strain prior to hypotonic stretch. (*B*) As in *A*, except the cells were loaded with the 20-mer antisense ODN. Data are representative of several similar experiments.

ref. 6). We used patch-clamp analysis in the cell-attached configuration to determine changes in the swelling-activated open channel activity (NP_o) in response to the antisense ODNs for α_{1C} and α_{1S} isoforms. Following 18 hr of CMS, a typical swelling-activated cation channel response to hypotonic swelling is illustrated in Fig. 4*A*. Occasional spontaneous stretch-activated cation channel activity was observed in "strained control" cells without application of exogenous strain as we

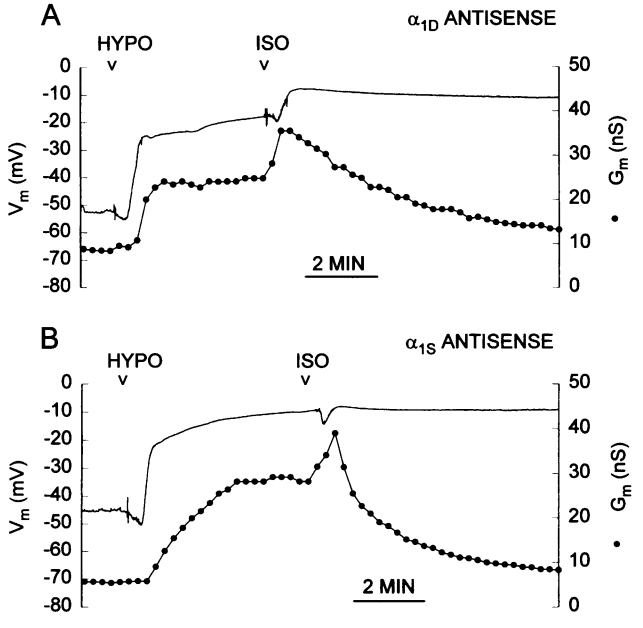

FIG. 3. Effect of antisense ODNs derived from the IV S_5–S_6 regions of the α_{1D} and α_{1S} genes on the response of V_m in G_m to hypotonic strain. (*A*) UMR-106.01 cell V_m and G_m response to hypotonic stretch and reversal by return to isotonic media. Cells were loaded with the ODN to the α_{1D} subunit gene and exposed to chronic, cyclic strain for 18 hr. (*B*) As in *A*, except the cells had been loaded with an antisense ODN to the α_{1S} subunit. Data are representative of several similar experiments.

have reported (6) (first trace, isotonic). Two minutes following perfusion of hypotonic Ringer's solution (182 mOsm) into the patch chamber, swelling-activated cation channel NP_o increased to a mean of 1.93 ± 0.32 (n = 12). Following washout of the hypotonic bath with normal Na Ringer's, NP_o remained high (isotonic, 2 min post). However, 10 min after washout of hypotonic Ringer's, channel activity was not different from baseline before hypotonic challenge, although a small percentage of cells still exhibited spontaneous channel activity (isotonic, 10 min post). When UMR-106.01 cells were treated with α_{1S} antisense ODN, NP_o of swelling-activated cation channels in response to hypotonic challenge was not significantly different (2.21 ± 0.71; n = 6) from control cells (Fig. 4*B*, 182 mOsm). Washout of the hypotonic Ringer's resulted in the return of volume-activated cation channel activity to baseline over 10 min (Fig. 4*B*, isotonic 2 min post and 10 min post). However, Fig. 4*C* demonstrates that the α_{1C} antisense ODNs (24-mer) eliminated the swelling-activated cation channel activity in response to hypotonicity (n = 6) (182 mOsm). The α_{1C} antisense ODN also eliminated stretch-activated cation channel activity. The results were exactly similar to Fig. 4*C* showing no channel activity induced by back pressure in the patch pipette (n = 20) and are not further illustrated. α_{1S} or α_{1D} antisense ODNs had no effect on stretch-activated cation channel activity, and the increased stretch-activated channel activity following CMS was as reported (6).

Gadolinium also inhibited the increase in swelling-activated cation activity in response to perfusion with 182 mOsm bath similar to its inhibition of the increase in stretch-activated cation channel activity following CMS (figure 4 in ref. 6). These data suggest that the inhibition of the swelling-induced increase in G_m following CMS may have been mediated through inhibition of increased swelling-activated cation channel activity.

Characterization of the swelling-activated cation channel activity by single channel recordings revealed that these channels were insensitive to changes in V_m, insensitive to nifedipine and nitrendipine and blockable by Gd^{3+}. Thus, in these characteristics, they were similar to stretch-activated cation channels of UMR-106.01 cells, which have been previously characterized (4). To determine whether the swelling-induced conductance in cells subjected to CMS was due to activation of stretch-activated cation channels, we measured the conductance and ion selectivity of single channels in inside-out patches activated by hypotonic swelling. When bathed in symmetrical or asymmetrical NaCl/KCl solutions (see *Materials and Methods*), the swelling-activated cation channels had a conductance of 28 pS, significantly greater than the 18 pS reported for stretch-activated cation channels (4). To further clarify the similarities and differences of the swelling-activated and stretch-activated ion channels, we determined the ion selectivity ratios for Na^+, K^+, Cl^-, and Ca^{2+}. When patches were bathed in asymmetrical NaCl/KCl solutions, the reversal potential of the *I–V* relation was not significantly different from 0 mV, indicating that the channel was equally conductive to both Na^+ and K^+ (Fig. 5*A*). These data indicate that the swelling-activated cation channel is nonselective for Na^+ and K^+ as is the stretch-activated cation channel described earlier (4). When bath solutions were changed from 138 mM NaCl to 65 mM NaCl/mannitol solutions, the reversal potential of the *I–V* relation was shifted to the right by 9.0 ± 1.0 mV (Fig. 5*A*). These data indicate that the swelling-activated cation channel has a P_{Na}/P_{Cl} of 5.5:1 and has, therefore, a relatively low selectivity for cations over anions. This is in contrast to the high cation selectivity of the stretch-activated cation channel which, under similar conditions, gives a rightward shift of the *I–V* relation of ≈17 mV, very close to the theoretical limit for a perfectly cation-selective channel (4). To determine the permeability of the channel to Ca^{2+}, we switched the bath solution to one containing 75 mM Ca^{2+} and fitted the resulting *I–V*

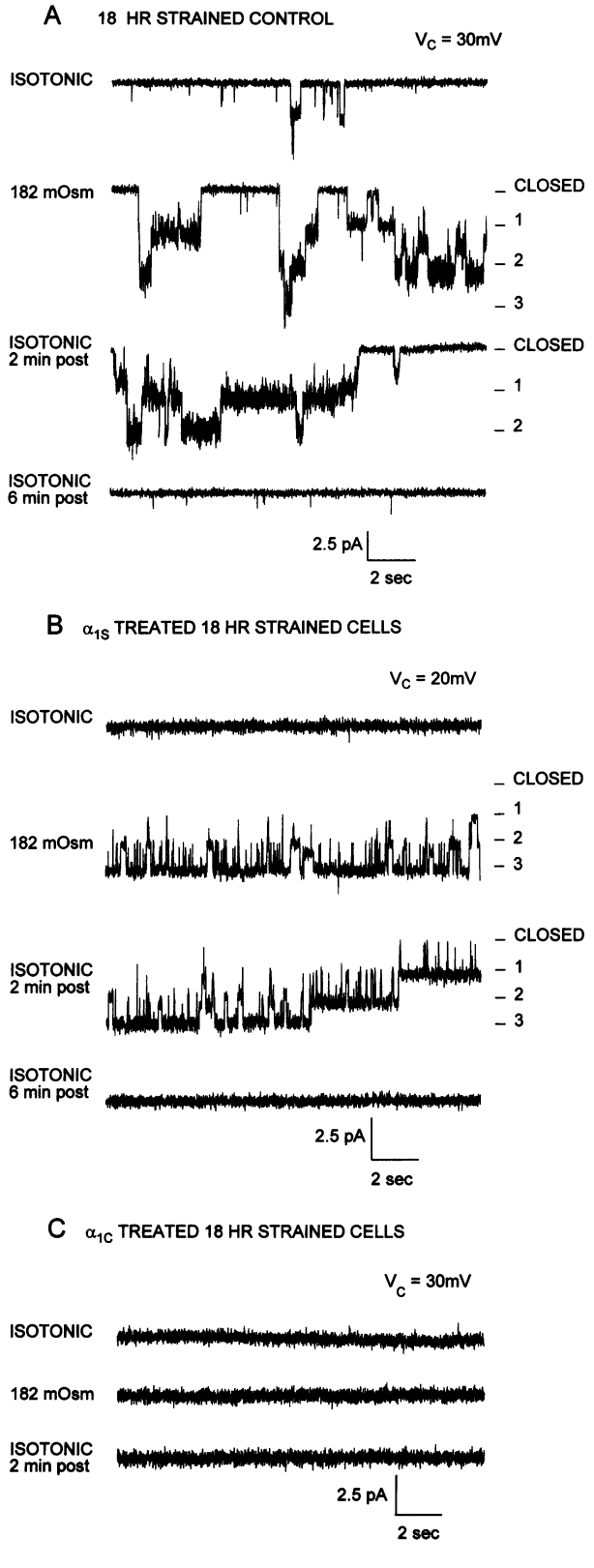

FIG. 4. Single channel recordings of swelling-activated cation channel activity in cells exposed to chronic, cyclic strain. (*A*) Swelling-activated cation channel activity after 18 hr of cyclic strain. Spontaneous swelling-activated cation channel activity and a high level of channel activity upon exposure to hypotonic media (182 mOsm) was observed. Upon return to isotonic media, there was decreased channel activity by 2 min and restoration to basal levels by 10 min. (*B*) Cells treated with antisense to α_{1S} and 18 hr of cyclic strain. Loading UMR-106.01 cells with the antisense ODN to the α_{1S} subunit gene failed to affect swelling-activated cation channel activity. Exposure to hypotonic media produced a major increase in channel activity, which returned to baseline following 10 min in isotonic media. (*C*) α_{1C} antisense-treated 18 hr strained cells. Failure to detect swelling-activated cation channel activity in UMR-106.01 cells loaded with the antisense ODN to the α_{1C} subunit in response to hypotonic stimulus.

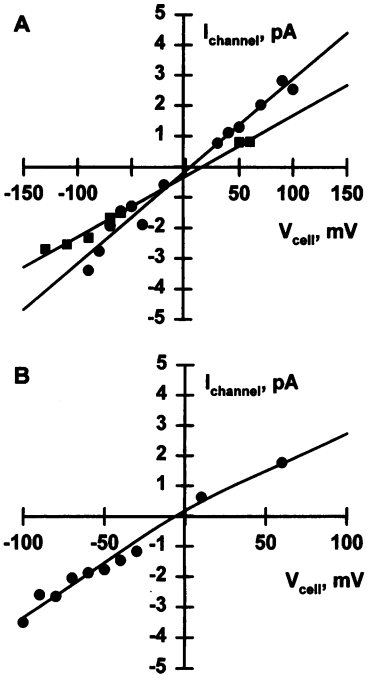

FIG. 5. Single swelling-activated cation channel current–voltage plots of excised patches bathed in asymmetrical solutions to determine channel ion selectivity. Lines represent fits of the data with the GHK current equation. (*A*) ●, Data obtained with 144 mM KCl in the pipette and 138 mM NaCl in the bath solution. Reversal potential of near zero indicates a 1:1 selectivity ratio for Na^+ and K^+. ■, Data obtained with 144 mM KCl in the pipette and 65 mM NaCl in the bath solution. Shift of reversal potential toward positive values indicates a 2.8:1 selectivity ratio of Na^+ to Cl^-. (*B*) Data obtained with 138 mM KCl in the pipette and 75 mM $CaCl_2$ in the bath solution. GHK fit indicates a P_{Ca}/P_{Na} of 0.6:1 and a P_{Na} of 3.9×10^{-8} cm/sec.

relation to a modified GHK equation (15) as shown in Fig. 5*B*. The P_{Na}/P_{Ca} was calculated to be 1.54:1 with $P_{Na} = 3 \times 10^{-8}$ cm/sec. It should be noted that the presence of Ca^{2+} on the cytosolic side of the patch had no effect on the permeability of the channel to Na^+. Channels in excised patches activated by swelling of UMR-106.01 cells subjected to CMS display a much lower sensitivity to pipette suction than do stretch-activated cation channels in cell-attached patches of the same cells in the absence of CMS. The stretch-activated cation channel is nearly completely activated by −30 mmHg suction on the patch pipette (4–6). The swelling-activated cation channels show little activation at 30 mmHg and typically required 60–80 mmHg suction to show a similar increase in NP_o.

DISCUSSION

In the studies reported here, we demonstrate that the response of chronically strained cells to hypotonic challenge is blocked by antisense ODNs to the α_{1C} subunit of the high-voltage, L-type calcium channel family (19). The α_1 subunit of this family of channels contains the channel pore, the voltage sensor, and the dihydropyridine receptor (11, 20–22). These data suggest that the swelling-activated cation channel, which is voltage insensitive and dihydropyridine insensitive and Gd^{3+} blockable, similar to the stretch-activated cation channel (4–6), may either contain homology to an α_1 subunit of the high-voltage L-type calcium channel family, or α_{1C} expression

is required for swelling-activated cation channel activation. Our data cannot distinguish between these possibilities, and resolution will require α_{1C} expression and reconstitution of activity experiments.

Failure of α_{1C} sense ODNs and α_{1S} and α_{1D} antisense ODNs to affect swelling-activated cation channel activity and G_m in response to CMS served as controls for the effect of the α_{1C} antisense ODNs. Antibodies were not available to analyze whether the ODN affected α_{1C} protein expression. However, Western blot analysis of the α_1 subunit levels has been difficult in most laboratories, so had we an antibody, this strategy probably would have not met with success. In many reports with antisense ODNs, investigators have been able to demonstrate reductions in the level of targeted mRNA. However, this is not a uniform observation due to additional mechanisms of ODN action besides RNase H activity (18, 24). The amount of ODNs needed to perform Northern blot analysis for α_{1C} in the presence of antisense was too great to be feasible because of the large amount of RNA required for Northern analysis (9), the amount of cells required for application to the strain apparatus, and the concentrations of unmodified phosphodiester ODN that we used. Therefore, we were unable to assess the effects of antisense ODN on α_{1C} message levels. However, the controls, based on failure of sense and α_{1S} and α_{1D} antisense to affect single channel activity and G_m, adequately demonstrate the specificity of the α_{1C} antisense ODN in eliminating swelling-activated cation channel activity and its adaptation to CMS. The ODNs used in the above studies were all unmodified phosphodiester ODNs. Thus, the streptolysin O permeabilization may have avoided expected degradation in culture media (18, 20, 24) and facilitated the superior sequence-specific effects of phosphodiester ODNs.

The antisense ODNs used in these studies were against the region 5′ of the S6 in domain IV. This region is upstream of the dihydropyridine receptor (23). Since the stretch-activated cation channel, the swelling-activated cation channel, and the strain-induced G_m increase are not inhibited by 10 μM nifedipine (6), the dihydropyridine receptor must not be expressed or is very insensitive to dihydropyridines in the isoform of the α_{1C}, which is being acted on by the antisense ODN. Furthermore, this isoform could have key divergences from other dihydropyridine-sensitive channels since the cation channel inactivated by antisense α_{1C} ODN is voltage independent and sensitive to Gd^{3+}. These trivalent cation-sensitive and cation nonselective characteristics suggest significant differences in the gene splicing between this isoform and others of the dihydropyridine-sensitive L-type calcium channels. Clarification of these issues requires reconstitution of swelling-activated cation channel activity with expression of the full-length α_{1C} protein. This will allow sequence structure–function analysis.

Finally, our data do not allow us to distinguish between stretch-activated and swelling-activated cation channels. There were significant similarities in the channel properties, but there were also differences in conductance and cation/anion selectivity. One possibility is that the effect of swelling on the cell (i.e., the cytoskeleton) differs from that of back pressure on the patch pipette. This is assuredly the case and, since the swelling-activated cation channels are sensitive to cytoskeletal disruption (R.L.D., unpublished observations), changes in channel characteristics could have been produced by the two different forces. The insensitivity of the swelling-activated channel to stretch may also be attributable to swelling-induced changes in the channel's relationship to the cytoskeleton. We have noted that cell-attached patches of hypotonically swollen UMR-106-01 cells subjected to CMS typically require −60 mmHg or greater pipette suction to measurably increase NP_o. This is in contrast to the stretch-activated cation channel, which shows maximal increase in NP_o at −30 mmHg (4–6).

In summary, we have shown that antisense ODNs directed against the α_{1C} subunit of the L-type calcium channel family specifically inhibit a swelling-activated, Gd^{3+}-sensitive cell conductance and both swelling-activated and stretch-activated, nonselective cation channels in cells subjected to CMS. While we cannot determine from our data that the swelling-activated and stretch-activated cation channels are subunits of the L-type calcium channel family, it is clear that the α_{1C} gene product is critical to the transduction of mechanical strain into a process that regulates transmembrane cation permeability.

The authors wish to thank Ms. Laura Harter for excellent technical assistance. This work was supported in part by the Monsanto Searle/Washington University Biomedical Program National Institutes of Health Grants R01 AR39561 (K.A.H.), NASA NAG2-791 (R.L.D.), and GM34399 (P.A.F.).

1. Biewener, A. A. & Bertram, J. E. A. (1993) in *Bone: Bone Growth B*, ed. Hall, K. (CRC, Melbourne, FL), Vol. 7, pp. 1–36.
2. Smith, E. L. & Gilligan, C. (1990) in *Osteoporosis: Physiological Basis, Assessment, and Treatment*, eds. DeLuca, H. F. & Mazess, R. (Elsevier Science, New York), pp. 285–293.
3. Simkin, A., Ayalon, J. & Leichter, I. (1987) *Calcif. Tissue Int.* **40,** 59–63.
4. Duncan, R. & Misler, S. (1989) *FEBS Lett.* **251,** 17–21.
5. Duncan, R. L., Hruska, K. A. & Misler, S. (1992) *FEBS Lett.* **307,** 219–223.
6. Duncan, R. L. & Hruska, K. A. (1994) *Am. J. Physiol.* **267,** F909–F916.
7. Morris, C. E. & Horn, R. (1991) *Science* **251,** 1246–1249.
8. Harter, L. V., Hruska, K. A. & Duncan, R. L. (1994) *Endocrinology* **136,** 1–7.
9. Barry, E. L. R., Gesek, F. A., Froehner, S. C. & Friedman, P. A. (1995) *Proc. Natl. Acad. Sci. USA* **92,** 10914–10918.
10. Birnbaumer, L., Campbell, K. P., Catterall, W. A., Harpold, M. M., Hofmann, F., Horne, W. A., Mori, Y., Schwartz, A., Snutch, T. P., Tanabe, T. & Tsien, R. W. (1994) *Neuron* **13,** 505–506.
11. Perez-Reyes, E., Kin, H. J., Lacerda, A. E., Horne, W., Wei, X., Rampe, D., Campbell, K. P., Brown, A. M. & Birnbaumer, L. (1989) *Nature (London)* **340,** 233–236.
12. Banes, A. J., Link, G. W., Gilbert, J. W., Tran Son Tay, R. & Monbureau, O. (1990) *Am. Biotech. Lab.* **8,** 12–23.
13. Barry, E. L. & Gesek, F. A. & Friedman, P. A. (1993) *Biotechniques* **15,** 10616–10620.
14. Horn, R. & Marty, A. (1988) *J. Gen. Physiol.* **92,** 145–159.
15. Lewis, C. A. (1979) *J. Physiol. (London)* **286,** 417–445.
16. Sokal, R. R. & Rohlf, F. J. (1981) *Biometry* (Freeman, New York).
17. Barry, E. L. R., Gesek, F. A. & Friedman, P. A. (1993) *J. Am. Soc. Nephrol.* **4,** 862 (abstr).
18. Stein, C. A. (1992) *Leukemia* **6,** 967–974.
19. Catterall, W. A., Seagar, M. J. & Takahashi, M. (1988) *J. Biol. Chem.* **263,** 3535–3538.
20. Biel, M., Ruth, P., Bosse, E., Hullin, R., Stuhmer, W., Flockerzi, V. & Hofmann, F. (1990) *FEBS Lett.* **269,** 409–412.
21. Tanabe, T., Takeshima, H., Mikami, A., Flockerzi, V., Takahasai, H., Kangawa, K., Kojima, M., Matsu, H., Hirse, T. & Numa, S. (1987) *Nature (London)* **328,** 313–318.
22. Mikami, A., Imoto, K., Tanabe, T., Niidome, T., Mori, Y., Takeshima, H., Narumiya, S. & Numa, S. (1989) *Nature (London)* **340,** 230–233.
23. Tsien, R. W., Ellinor, P. T. & Horne, W. A. (1991) *Topics Physiol. Sci.* **12,** 349–354.
24. Bennett, C. F. & Crooke, S. T. (1994) *Adv. Pharmacol.* **28,** 1–43.
25. Perez-Reyes, E., Wei, X., Castellano, A. & Birnbaumer, L. (1990) *J. Biol. Chem.* **265,** 20430–20436.